DOI:10.13476/j.cnki.nsbdqk.2020.0071
姜欣彤,黎曙,周祖昊,等.基于高程分段的黄河源区 NDVI 和水热条件空间分布格局[J].南水北调与水利科技(中英文),2020,18(4):39-53. JIANG X T,LI S,ZHOU Z H,et al. Distribution pattern of NDVI and hydrothermal conditions in the Yellow River Headwaters based on elevation section[J]. South-to-North Water Transfers and Water Science & Technology,2020,18(4):39-53. (in Chinese)

基于高程分段的黄河源区 NDVI 和水热条件空间分布格局

姜欣彤[1,2],黎曙[3],周祖昊[2],庞亮[1],严子奇[2],蓝云龙[3],朱家松[4]

(1.中国海洋大学 工程学院,山东 青岛 266100;2.中国水利水电科学研究院 流域水循环模拟与调控国家重点实验室,北京 100038;3.黄河水利委员会 西宁水文水资源勘测局,西宁 810008;4.深圳大学 土木工程学院,深圳 518000)

摘要:以黄河源区植被为研究对象,应用 MODIS13Q1 遥感数据、DEM 数据、气象数据以及土地利用类型图,采用基于高程分段的研究方法对研究区 NDVI(归一化植被指数)与水热条件空间分布特征进行深入探究。根据 NDVI 随高程分布特征,将研究区划分为高程段Ⅰ(<3 400 m),高程段Ⅱ(3 400~4 200 m)和高程段Ⅲ(>4 200 m)。在各高程段内分析植被分布格局、NDVI 与水热条件分布特征、NDVI 与水热因子响应关系。结果表明:黄河源区内主要植被类型为草地,其面积占源区总面积 75%,林地面积占比为 7%,农田面积仅占 1%;高程段Ⅰ内主要植被类型为农田和草地,高程段Ⅱ内主要植被类型为林地和草地,高程段Ⅲ内基本只有草地;3 种不同类型植被 NDVI 平均值大小为林地>草地>农田;气温表现为梯度递减的空间分布格局,降水量呈现从东南向西北递减的趋势;高程段Ⅰ属干旱区域,高程段Ⅱ属湿热区域,高程段Ⅲ属干冷区域;3 个高程段内水热组合条件最好的是高程段Ⅱ,高程段Ⅲ水热条件较差;植被 NDVI 在不同高程段内受水热因子的驱动作用不同;高程段Ⅰ和高程段Ⅲ内降水量较低,NDVI主要驱动因子是降水量,高程段Ⅱ的降水量丰沛,影响 NDVI 的主要因子是气温。

关键词:NDVI;水热条件;空间分布格局;黄河源区;高程分段

中图分类号:P339 **文献标志码**:A **开放科学(资源服务)标志码(OSID)**:

气候变化、植被变化及其水文效应是目前国际科学社会的热点问题,也是水资源利用及生态工程建设中的基础科学问题[1]。黄河源区作为黄河的“水塔”,其生态环境质量对下游地区的生态环境有重要的影响,对黄河源区植被状况、气候条件及其响应关系的研究具有重要意义。针对黄河源区气候与植被变化的研究,有学者得出结论,气候因素对黄河源区植被生长变化起到主要的促进作用[2],自 20 世纪 80 年代后期开始黄河源区气候由“暖干”转向“暖湿”[3],源区内植被生长呈改善趋势[4]。针对黄河源区植被与气候因子的响应关系,有学者[5]认为降水是影响黄河源区植被生长的主导因子,也有学者[6]认为黄河源区植被覆盖对气温变化的响应更为敏感。由于黄河源区地形复杂,高差显著,在已有的研究中,尚未充分考虑到黄河源区的特点,分不同高程段研究 NDVI 在不同区域的分布特征。基于此,本文将研究区划分为不同高程段,探究不同高程段内植被分布特点,水热条件分布特点,及 NDVI 与水

收稿日期:2020-03-16 **修回日期**:2020-04-10 **网络出版时间**:2020-04-14
网络出版地址:http://kns.cnki.net/kcms/detail/13.1430.TV.20200414.1407.002.html
基金项目:国家重点研发计划(2016YFC0402405);国家自然科学基金(51779270);流域水循环模拟与调控国家重点实验室课题(SKL2018TS04)
作者简介:姜欣彤(1993—),女,吉林通化人,主要从事遥感水文学研究。E-mail:JXT_OUC@163.com
通信作者:周祖昊(1975—),男,湖北武汉人,教授级高级工程师,博士,主要从事流域水循环及伴生过程模拟与调控研究。E-mail:zhzh@iwhr.com

热因子响应关系的差异性。

1　数据与方法

1.1　研究区概况

黄河源区地势西高东低,西抵巴颜喀拉山,东抵岷山,南达邛崃山,北抵共和盆地,黄河环绕阿尼玛卿山,最后到达龙羊峡水库[7],总面积约为 13 万 km^2,地理坐标范围为 32°09′～36°34′N,95°54′～103°24′E。黄河源地区为 NW-SE 带状盆地地貌,地貌以高原平地、山地和丘陵台地为主,海拔在 2 438～6 169 m,平均海拔 4 473 m,为高海拔盆地[8]。黄河源区内自然环境类型多样,高寒植被分布广泛,植被类型以高寒灌丛、高寒草甸、高寒草原为主[9]。

1.2　数据来源及处理

本文所用归一化植被指数(NDVI)数据为美国 NASA 航天中心发布的 2003—2017 年 MOD13Q1 产品,时间分辨率为 16 d,空间分辨率为 1 km。利用 MRT(MODIS reprojection tool)技术将遥感影像进行数据拼接和重投影,提取 NDVI 波段并在 ArcGIS 中进行掩膜提取。由于黄河源区存在河流、湖泊、岩石和裸土等地表景观,其 NDVI 值小于 0,因此利用 ArcGIS 中栅格计算工具在数据预处理的基础上剔除掉非植被区域,将 NDVI 小于 0 的像元设置为空值。最后根据 MVC(max value composition)月最大合成法得到每月 NDVI 值。4—10 月是黄河源区植被生长季,本文将每年 4—10 月 NDVI 值计算平均值作为该年植被生长季 NDVI,2003—2017 年生长季多年平均 NDVI 空间分布见图 1(a)。

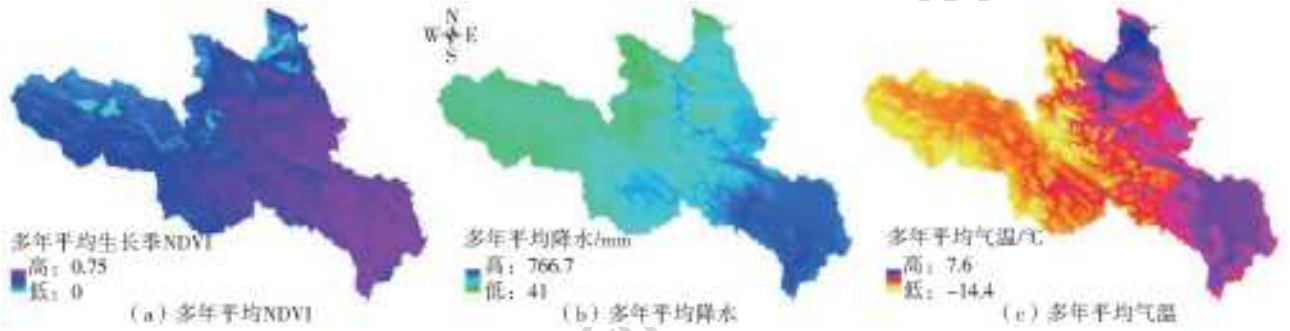

图 1　NDVI、降水、气温多年平均空间分布

本文所用气象数据为研究区内 12 个监测站点 2003—2017 年的气温、降水数据。黄河源区位于青藏高原东部,地形高差显著,降水和气温均具有明显的垂直分布特征[10],因此采用基于 DEM 的高程修正方法结合 IDW(inverse distance weighted)对气象数据进行处理[11]。在利用监测站点观测数据对气温空间插值时,气温垂直递减率是空间插值精度的重要影响因素[12]。利用研究区内 12 个监测站点多年平均气温 $\overline{T}$ 与站点高程(h)建立一元线性回归模型(图 2),由图可知多年平均气温 $\overline{T}$ 与站点高程回归模型方程为 $\overline{T}=-0.005\,5h+21.41$,$R^2$ 为 0.867 6,从而确定出气温的垂直递减率每 100 m 为−0.55 ℃。

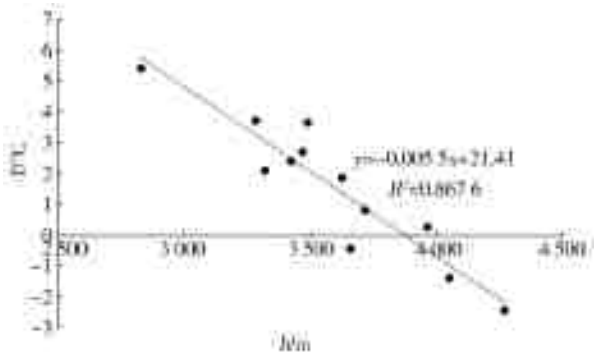

图 2　多年平均气温与监测站点高程回归模型

我国西北部地区的年降水量随海拔高度的升高而增加,变化幅度约为 1～18.13 mm/m[13],有研究[14-15]表明青藏高原降水具有梯度变化,东部区域每升高 100 m 降水增加 6～22 mm,郝振纯[16]对黄河源区雨量站进行分析得出降水的垂直变化率为+20 mm/m,故本文将降水垂直变化率选定为+20 mm/m。根据气温和降水垂直变化率,将监测站数据订正到大地水准面上,在 ArcGIS 中采用反距离权重法(IDW)对监测站点数据进行空间插值。结合 30 m 精度的 DEM 数据,将大地水准面上的气温降水数据订正为正常高程的气温降水数据。2003—2017 年多年平均降水和多年平均气温空间分布见图 1(b)、1(c)。

1.3　相关性分析

对 2003—2017 年黄河源区生长季 NDVI 与气温降水进行相关性分析,相关系数记为

$$R=\frac{\sum_{i=1}^{n}(X_i-\overline{X})(Y_i-\overline{Y})}{\sqrt{\sum_{1=1}^{n}(X_i-\overline{X})^2\sum_{i=1}^{n}(Y_i-\overline{Y})^2}} \tag{1}$$

式中:X_i 表示第 i 年 NDVI,即 2003—2017 年生长季 NDVI 值;$\overline{X}$ 表示 NDVI 生长季多年平均值;Y_i 表示第 i 年气温/降水;$\overline{Y}$ 表示多年平均气温/降水

量；n 表示研究时段年限 $n=15$。

采用 t 检验[17]对相关性进行显著性检验，计算公式为

$$t=R\Big/\sqrt{\frac{1-R^2}{n-2}} \tag{2}$$

式中：t 为检验统计度；R 为相关系数。根据相关系数及显著性检验将等级划分为 5 个等级[18]。极显著负相关($R<0$，$P\leqslant 0.01$)，显著负相关($R<0$，$0.01<P\leqslant 0.05$)，不显著相关($P>0.05$)，显著正相关($R>0$，$0.01<P\leqslant 0.05$)，极显著正相关($R>0$，$P\leqslant 0.01$)。

1.4　高程段划分

为研究黄河源区内 NDVI 分布随高程变化呈现的空间分带特征，采用 ArcGIS 工具在研究区内等间距选取样本点，提取样本点位置所在高程和植被生长季多年平均 NDVI 值，得到研究区 NDVI 随高程的变化图(图 3(a))。可以看出，NDVI 先呈现随着高程增加而增加的趋势，到某一海拔高度后 NDVI 值剧增，之后随着高程增加有缓慢减小的趋势，到某一海拔高度后出现大幅度减小且分布散乱的特征。为寻找 NDVI 随高程突变点，采用 t 检验法做突变分析。双总体 t 检验法是通过考察两组非相关样本序列平均值的差异是否显著来检验突变的方法[19]。如果两组样本序列均值的差异性超过了显著水平，则认为这两组样本发生了突变。其检验统计量 t 的计算公式为

$$t=\frac{\overline{X}_1-\overline{X}_2}{\sqrt{\dfrac{(n_1-1)S_1^2+(n_2-1)S_2^2}{n_1+n_2}\left(\dfrac{1}{n_1}+\dfrac{1}{n_2}\right)}} \tag{3}$$

式中：S_1^2 和 S_2^2 为两样本的方差，n_1 和 n_2 为两组样本容量 $\overline{X}_1$ 和 $\overline{X}_2$ 为两样本的平均值。将样本点 NDVI 值每 100 m 高程分为一组，每两组样本点进行 95% 置信水平的双总体 t 检验，以此检测 NDVI 随高程突变点。由图 3(b)可见，在高程3 300～3 400 m 和 4 100～4 200 m 时，两组 NDVI 值有显著性差异，即认为，NDVI 在高程3 400 m 和4 200 m 处发生突变。因此，将高程3 400 m 设置为高程段划分的第一条分界线，将高程4 200 m 设置为高程段划分的第二条分界线，这样将整个黄河源区按照 NDVI 随高程分布特点划分成 3 个高程段即高程段Ⅰ(<3 400 m)、高程段Ⅱ(3 400～4 200 m)和高程段Ⅲ(>4 200 m)。

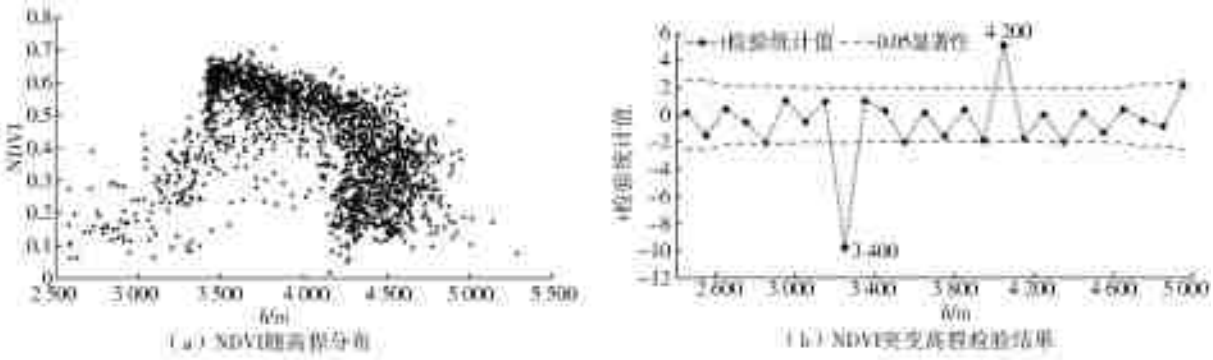

(a) NDVI随高程分布　　(b) NDVI突变高程检验结果

图 3　NDVI 随高程变化及突变检测结果

研究区高程分段见图 4。高程小于3 400 m 的区域主要位于研究区东北部，此区平均高程为 3 105 m，面积为9 137 km²，占流域总面积 7%，NDVI 分布在[0.03，0.5]内，平均值为 0.26；高程在3 400～4 200 m 的区域主要位于研究区东南部，此区平均高程为3 731 m，面积为57 744 km²，占流域总面积 45%，NDVI 分布在[0.26，0.66]内，平均值为 0.55；高程大于4 200 m 的区域位于研究区西北部，此区平均高程为4 441 m，面积为62 094 km²，占流域总面积 48%，NDVI 分布在[0.09，0.56]内，平均值为 0.34。

图 4　高程分区空间示意图

2　结果与讨论

2.1　不同高程段植被分布格局

研究 NDVI，首先应了解研究区内植被的分布情况。选取 2000 年和 2015 年两期土地利用类型图做转移矩阵分析，结果表明林地和农田面积变化均不超过 0.1%，草地面积变化不超过 2%，可以认为 2003—2017 年黄河源区土地利用变化不大，故本文采用 1 km 精度的 2015 年作为典型年对黄河源区土地利用类型(图 5)加以分析。由图 5 可以看出黄

河源区的植被类型为草地、林地和农田。对土地利用类型面积占比进行统计得出,草地为黄河源区主要植被类型,面积占整个研究区面积 75%;其次是林地,面积占整个研究区面积 7%;东北部分布着少量农田,其面积只占整个研究区面积的 1%。将土地利用类型图与高程分区叠加,得到不同高程分区内的不同植被类型面积占比(图 6)。从植被类型分布上看:高程段Ⅰ内植被面积(林、草、田)共占土地利用总面积的 73.39%,农田和草地是该区域的主要植被类型,面积比重分别为 16.79%和 79.46%,林地占 3.75%;高程段Ⅱ内植被面积占土地利用总面积的 87.52%,主要植被类型为林地和草地,面积比重分别为 14.25%和 85.61%;高程段Ⅲ内植被面积占土地利用总面积的 78.82%,其中 97.02%的植被都是草地,林地仅占 2.98%。

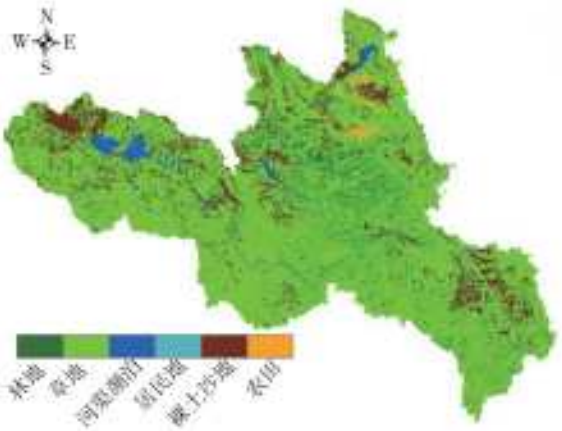

图 5　2015 年研究区土地利用类型图

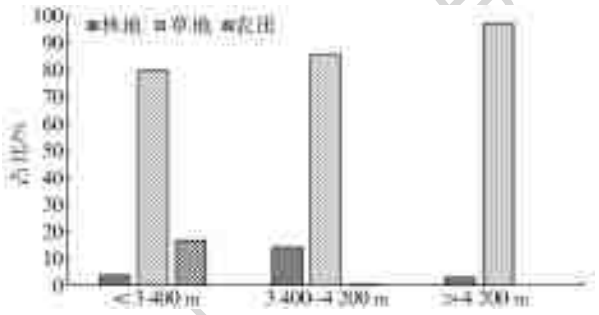

图 6　不同高程段内不同植被类型占比

NDVI 数据与植被的许多参数密切相关,能够反映出植被差异及植被长势[20],因此不同类型的植被 NDVI 也具有差异性。核密度估计概率分布是一种非参数估计方法,能够反映样本的分布情况[21]。为探究不同类型的植被 NDVI 分布特点,提取 3 种类型植被(林地—L,草地—C,农田—T)生长季多年平均 NDVI 值分别做核密度估计分布图(图 7)。通过对比可以看出:林地的 NDVI 平均值最高,为 0.52;其次是草地的 NDVI 平均值为 0.43;农田 NDVI 平均值最小,为 0.32。3 种植被 NDVI 分布特点也具有差异性,林地 NDVI 分布较为集聚,草地 NDVI 分布较为均匀且跨度较大,农田 NDVI 分布接近正态分布。按照 95%置信区间确定上下限,则林地 NDVI 分布范围为[0.27,0.65],草地 NDVI 分布范围为[0.14,0.64],农田 NDVI 分布范围为[0.13,0.57]。由此可见,植被类型分布的区域差异性造成了 NDVI 随高程变化的特点:高程段Ⅰ内的 NDVI 主要反映了农田和草地的长势,NDVI 值较小;高程段Ⅱ内的 NDVI 主要反映了林地和草地的长势,因此 NDVI 值较高;高程段Ⅲ内的 NDVI 基本只反映草地的长势,因此 NDVI 分布较散乱,跨度大。由此可以解释 NDVI 在黄河源区 3 个高程段内的分布特点。

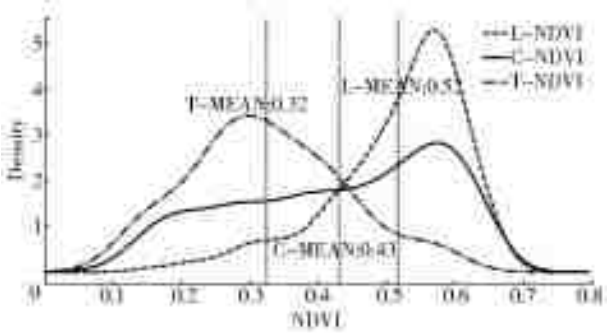

图 7　林地、草地、农田核密度估计分布

2.2　不同高程段水热条件分布格局

降水和气温是影响地表植被覆盖的两个重要的气象要素[22]。为深入探究黄河源区 NDVI 空间分布差异成因,分别做 3 个高程段内 2003—2017 年多年平均水热条件联合分布图,降水和气温集中分布在颜色较深的区间(图 8)。经过对比发现:高程段Ⅰ降水分布范围为(286 mm,587 mm),但集中分布在 400~500 mm,平均降水量为 455 mm,气温分布范围为(1.5 ℃,6.9 ℃),集中分布在 3~5 ℃;高程段Ⅱ降水分布范围为(320 mm,717 mm),平均值为 553 mm,分布较为均匀,气温分布范围为(-3.2 ℃,3.08 ℃),分布跨度较大,且呈现双峰型,集中分布在(2~4 ℃)和(-1~1 ℃),平均值为 0.34 ℃;高程段Ⅲ降水的分布范围为(241 mm,533 mm),平均值为 377 mm,在 250~350 mm 区间分布较为集中,气温分布范围为(-6.6 ℃,-1.7 ℃),平均温度为-3.87 ℃。气温表现为梯度递减的空间分布格局,可以看出随着高程增加热量条件服从海拔递减规律。降水量在高程段Ⅱ内最为充沛,在高程段Ⅲ内最少,降水呈现从东南向西北递减的趋势,这是因为印度洋和太平洋是青藏高原东部主要水汽来源地[23]。从水热组合条件来看:高程段Ⅰ温度高,降水少,属干旱区域;高程段Ⅱ、温度高,降水多,属湿热区域;高程段Ⅲ温度低,降水少,属干冷区域。3 个高程段水热组合条件最好的是高程段Ⅱ,其次是高程段Ⅰ,高程段Ⅲ内的水热条件较差。

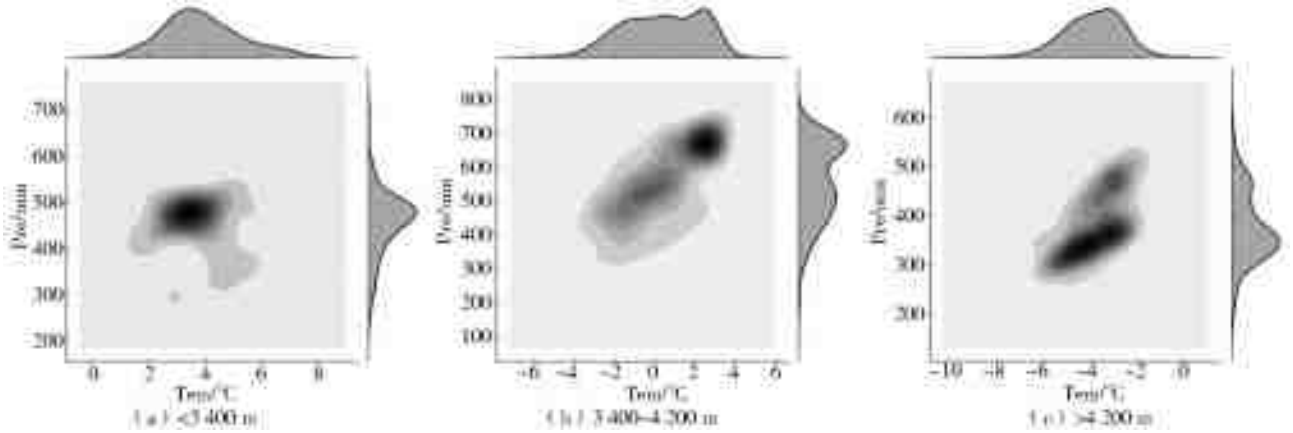

图 8　不同高程段水热条件分布特征对比

2.3　不同高程段 NDVI 与水热因子响应

将 2003—2017 年逐年 NDVI 值与气温、降水量分别做相关分析，并采用 t 检验方法对其显著性进行检验，不同高程段内 NDVI 与水热因子的相关性空间分布图和统计结果见图 9、10。结果表明，就流域总体而言，大多数区域生长季植被与气候因子表现为不显著相关或显著正相关，呈显著负相关的区域极少，几乎没有区域呈极显著负相关。对于不同高程段，对 NDVI 有显著影响的因子有所不同。高程段Ⅰ内 NDVI 与降水量呈极显著、显著正相关的区域占 59.3%，但仅有 4.3%的区域 NDVI 与气温呈极显著、显著正相关；高程段Ⅱ内有 12.6%的区域 NDVI 与降水量呈极显著、显著正相关，但与气温呈极显著、显著正相关的区域却占 44.1%；高程段Ⅲ内有 43.4%的区域 NDVI 与降水量呈极显著、显著正相关，但与气温呈极显著、显著正相关的区域仅有 8.2%。三个高程段内，高程段Ⅰ与高程段Ⅲ展现出了相似的特点，即 NDVI 与降水量的相关性较好，与气温的相关性较差，而高程段Ⅱ展现出了相反的特点，NDVI 与气温的相关性要高于与降水量的相关性。

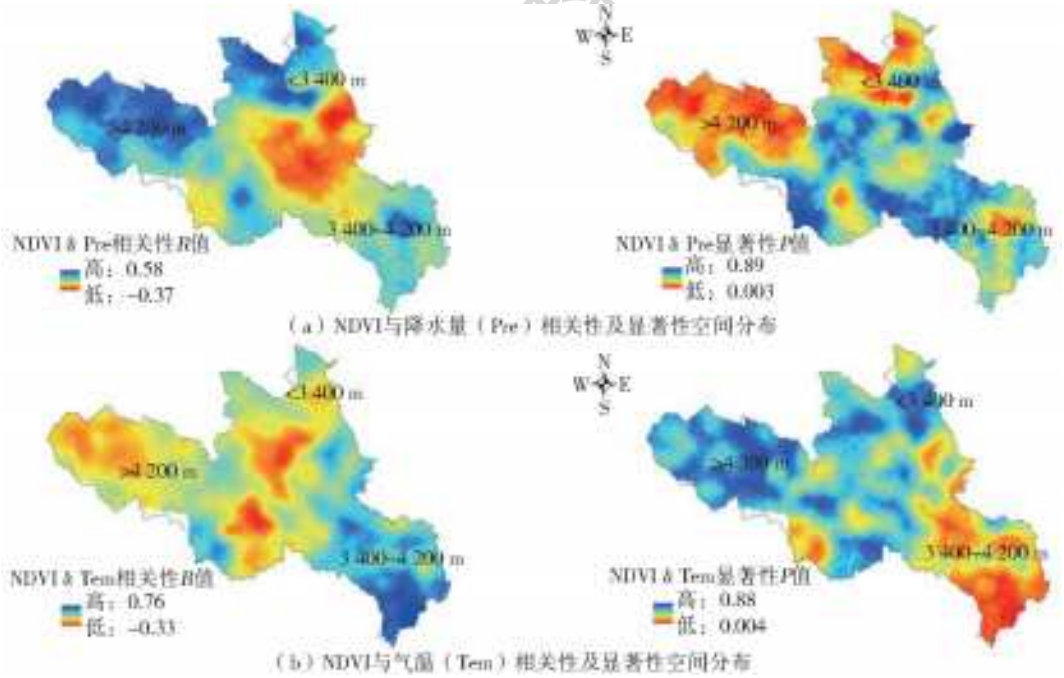

图 9　NDVI 与水热因子相关性及显著性空间分布

结合上文对三个高程段内水热条件分布格局的分析可以发现，自然条件不同，植被 NDVI 受水热因子的驱动作用不同。降水量较低的高程段Ⅰ和高程段Ⅲ内 NDVI 主要受降水因子的影响，降水量丰沛的高程段Ⅱ影响 NDVI 的主要因子是气温。产生这种结果的原因可能是由于北部的高程段Ⅰ区和高程段Ⅲ气候干旱、水分匮乏、土壤水分含量低，植被生长受水分限制较大，降水量的增加能够增加土壤湿度，为植被的生长提供充足的水分，促使植物进行光合作用，因此这两个高程区内 NDVI 与降水量呈现正相关特征。对于降水量非常充足的高程段Ⅱ，土壤水分含量高，植被的生长将不受水分条件的限制，降水量对植被的生长状况影响就会减弱，此时气温就会成为影响植被生长的主要因子。

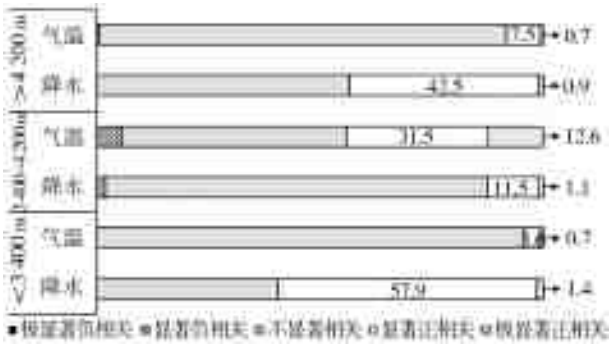

图 10　NDVI 与水热因子相关性统计结果

3　结　论

本文根据 NDVI 随高程变化趋势对研究区进行高程段划分，探讨了不同高程段内的植被分布类型、水热组合条件分布特征以及 NDVI 与水热因子的相关性，主要结论如下。

(1)高程段Ⅰ的主要植被类型农田和草地，高程段Ⅱ内主要植被类型为林地和草地，高程段Ⅲ内基本只有草地。3 种不同植被类型 NDVI 具有不同的分布特点，林地 NDVI 分布较为集聚，草地 NDVI 分布较为均匀且跨度较大，农田 NDVI 分布接近正态分布，其平均值大小为林地＞草地＞农田。(2)黄河源区整体气温表现为梯度递减的空间分布格局，降水量呈现从东南向西北递减的趋势。高程段Ⅰ温度高，降水量少，属干旱区域；高程段Ⅱ温度高，降水量多，属湿热区域；高程段Ⅲ温度低，降水量少，属干冷区域。高程段Ⅱ水热组合条件最好，其次是Ⅰ区，高程段Ⅲ水热条件较差。(3)不同高程段因其独特的自然条件，植被 NDVI 受水热因子的驱动作用不同。降水量较低的高程段Ⅰ和高程段Ⅲ NDVI 主要受降水因子的影响，降水量丰沛的高程段Ⅱ影响 NDVI 的主要因子是气温。

参考文献：

[1] 何霄嘉，王国庆，鲍振鑫. 气候、植被变化与水文循环响应研究进展及展望[J]. 水资源与水工程学报，2016，27(2)：1-5. DOI：10. 11705/j. issn. 1672-643X. 2016. 02. 01.

[2] 刘启兴，董国涛，景海涛，等. 2000－2016 年黄河源区植被 NDVI 变化趋势及影响因素[J]. 水土保持研究，2019，26(3)：86-92. DOI：10. 13869/j. cnki. rswc. 2019. 03. 013.

[3] 蓝永超，鲁承阳，喇承芳，等. 黄河源区气候向暖湿转变的观测事实及其水文响应[J]. 冰川冻土，2013，35(4)：920-928. DOI：10. 7522/j. issn. 1000 0240. 2013. 0104.

[4] 徐浩杰，杨太保，曾彪. 黄河源区植被生长季 NDVI 时空特征及其对气候变化的响应[J]. 生态环境学报，2012，21(7)：1205-1210. DOI：10. 3969/j. issn. 1674-5906. 2012. 07. 005.

[5] 史丹丹，杨涛，胡金明，等. 基于 NDVI 的黄河源区生长季植被时空变化及其与气候因子的关系[J]. 山地学报，2018，36(2)：184-193. DOI：10. 16089/j. cnki. 1008-2786. 000314.

[6] 吴喜芳，李改欣，潘学鹏，等. 黄河源区植被覆盖度对气温和降水的响应研究[J]. 资源科学，2015，37(3)：512-521.

[7] 胡光印，金会军，董治宝，等. 黄河源区土地利用/覆盖变化(LUCC)研究[J]. 冰川冻土，2014，36(3)：573-581. DOI：10. 7522issn. 10000240. 2014. 0068.

[8] 钱程，韩建恩，朱大岗，等. 基于 ASTER-GDEM 数据的黄河源地区构造地貌分析[J]. 中国地质，2012，39(5)：1247-1260. DOI：10. 3969/j. issn. 1000-3657. 2012. 05. 012.

[9] 陈琼，周强，张海峰，等. 三江源地区基于植被生长季的 NDVI 对气候因子响应的差异性研究[J]. 生态环境学报，2010，19(6)：1284-1289. DOI：10. 3969/j. issn. 1674-5906. 2010. 06. 004.

[10] 张杰，李栋梁，何金梅，等. 地形对青藏高原丰枯水年雨季降水量空间分布的影响[J]. 水科学进展，2007(3)：319-326. DOI：10. 3321/j. issn：1001-6791. 2007. 03. 002.

[11] 崔晓临，程贇，张露，等. 基于 DEM 修正的 MODIS 地表温度产品空间插值[J]. 地球信息科学学报，2018，20(12)：1768-1776. DOI：10. 12082/dqxxkx. 2018. 180340.

[12] 蔡迪花，郭铌，李崇伟. 基于 DEM 的气温插值方法研究[J]. 干旱气象，2009，27(1)：10-17. DOI：10. 3969/j. issn. 1006-7639. 2009. 01. 002.

[13] 玄海燕，罗双华. 我国区域降水量与海拔高度关系的分析[C]. 中国现场统计研究会第十三届学术年会论文集，2007：110-113.

[14] 鲁春霞，王菱，谢高地，等. 青藏高原降水的梯度效应及其空间分布模拟[J]. 山地学报，2007(6)：655-663. DOI：10. 3969/j. issn. 1008-2786. 2007. 06. 003.

[15] 鲁春霞，于格，郭广猛，等. 青藏高原降水的梯度效应及其水塔功能[C]. 2005 青藏高原环境与变化研讨会论文摘要汇编，2005：17.

[16] 郝振纯，张越关，杨传国，等. 黄河源区水文模拟中地形和融雪影响[J]. 水科学进展，2013，24(3)：311-318.

[17] 陈彦光. 地理数学方法[M]. 北京：科学出版社，2011.

[18] GAO Q Z，LI Y，WAN Y F，et al. Dynamics of alpine grassland NPP and its response to climate change in northern Tibet[J]. Climatic Change，2009，97(3-4)：515. DOI：10. 1007/s10584-009-9617-z.

[19] 魏凤英. 现代气候统计诊断与预测技术[M]. 北京：气象出版社，2007.

[20] 陈朝晖，朱江，徐兴奎. 利用归一化植被指数研究植被分类、面积估算和不确定性分析的进展[J]. 气候与环境研究，2004(4)：687-696. DOI：10. 3969/j. issn. 1006-9585. 2004. 04. 013.

[21] NA L，QIAN F. Multi-objective evolutionary of distribution algorithm using kernel density estimation model [C]. Proceedings of the 8th World Congress on Intelligent Control and Automation. 2010：2843-2848. DOI：10. 1109/WCICA. 2010. 5554745.

[22] 徐兴奎，林朝晖，薛峰，等. 气象因子与地表植被生长相关性分析[J]. 生态学报，2003(2)：221-230. DOI：10. 3321/j. issn：1000-0933. 2003. 02. 001.

[23] 张文江，高志强. 青藏高原中东部水热条件与 NDVI 的空间分布格局[J]. 地理研究，2006(5)：877-886. DOI：10. 3321/j. issn：1000-0585. 2006. 05. 01.

·译文(Translation)·

DOI:10.13476/j.cnki.nsbdqk.2020.0071

Distribution pattern of NDVI and hydrothermal conditions in the Yellow River Headwaters based on elevation section

JIANG Xintong[1,2], LI Shu[3], ZHOU Zuhao[2], PANG Liang[1], YAN Ziqi[2], LAN Yunlong[3], ZHU Jiasong[4]

(1. Engineering College, Ocean University of China, Qingdao 266100, China; 2. State Key Laboratory of Simulation and Regulation of Water Cycle in River basin, China Institute of Water Resources and Hydropower Research, Beijing 100038, China; 3. Xining Hydrology and Water Resources Survey Bureau of Yellow River Conservancy Commission, Xining 810008, China; 4. Civil Engineering College, Shenzhen University, Shenzhen 518000, China)

Abstract: Different datasets (MODIS13Q1 NDVI, DEM, LULC, and meteorological data) were used to study the regional differences of the spatial distribution pattern of NDVI and hydrothermal conditions in the Yellow River Headwaters. The distribution pattern of vegetation and hydrothermal conditions and the correlation between NDVI and hydrothermal factors were analyzed and investigated based on three elevation sections (section I<3 400 m, section II 3 400 m~4 200 m, section III>4 200 m), respectively. The results showed that: the main type of vegetation in the Yellow River Headwaters was grassland, which accounted for 75% of the total area. However, forest and farmland areas accounted for 7% and 1%, respectively; farmland was mainly distributed in section Ⅰ and the forest was mainly distributed in section Ⅱ, while grass grows in all three sections; the average NDVI of different vegetation types ranks in this order: forest, grassland, and farmland; moreover, the temperature displayed a spatial distribution pattern of decline gradient, and the precipitation represented a declining trend from southeast to northwest; the three partitions have different hydrothermal conditions, section I belonged to the arid region, section II belonged to the moist-heat region, and section Ⅲ belonged to the dry region, respectively; section Ⅱ had the relatively best hydrothermal combination conditions, which was followed by section Ⅰ, while section Ⅲ had the worst of three partitions; the results also revealed that NDVI was driven by different hydrothermal factors in different sections; the main factor that affected the growth of vegetation in section I and Ⅲ was precipitation, while in section II, the temperature is the main factor while the rainfall was abundant.

Key words: NDVI; hydrothermal condition; distribution pattern; Yellow River Headwaters; elevation section

Climate change, vegetation change, and its hydrological effects have become the hot issues of social concern in the international scientific community, which is also a basic scientific problem in water resource utilization and ecological engineering construction[1]. As the "water tower" of the

Received: 2020-03-16 **Revised**: 2020-04-10 **Online publishing**: 2020-04-14
Online publishing address: http://kns.cnki.net/kcms/detail/13.1430.TV.20200414.1407.002.html
Funds: National Key Research and Development Program(2016YFC0402405); National Natural Science Foundation of China(51779270); National Key Laboratory Project on Watershed Water Cycle Simulation and Regulation(SKL2018TS04)
Author brief: JIANG Xintong(1993-), female, Tonghua Jilin Province, engaged in remote sensing hydrology research. E-mail: JXT_OUC@163.com
Corresponding author: ZHOU Zuhao(1975-), male, Wuhan Hubei Province, engaged in the research on the simulation and regulation of watershed water cycle and associated processes, is a professor-level senior engineer with doctoral degree. E-mail: zhzh@iwhr.com

Yellow River, the ecological environment quality of the Yellow River Headwaters has an important impact on the ecological environment of the downstream region. Therefore, it is of great significance to study the vegetation status, climate conditions and their response relationship in the Yellow River Headwaters. The climatic factors play a major role in promoting vegetation growth[2]. Studies have shown that the climate pattern of the Yellow River Headwaters has changed from "warm and dry" to "warm and wet" since the late 1980 s[3], and the vegetation growth in the Yellow River Headwaters represents an improvement trend[4]. Researching on the response relationship between vegetation and climate factors in the Yellow River Headwaters, some scholars consider the precipitation as the main factor affecting vegetation growth[5], while others consider that vegetation cover is more sensitive to temperature change[6]. Given the complex topography and significant elevation difference in the Yellow River Headwaters, the distribution pattern of NDVI in different elevation sections has not been fully considered in the previous researches. In this study, the study area was divided into different elevation sections according to the vegetation distribution with elevation. The distribution pattern of vegetation, the hydrothermal conditions, and the correlation between NDVI and hydrothermal factors will be investigated in different elevation sections.

1 Materials and methods

1.1 Study area

The Yellow River Headwaters has a terrain of high in the west and low in the east, reaching Bayan Har Mountain in the west, Minshan Mountain in the east, Qionglai Mountain in the south, and Gonghe Basin in the north, surrounding Anemaqing Mountain with the Tangnaihai station as the outlet of the catchments[7]. The catchments are located in the region between 32°09′ and 36°34′N and between 95°54′ and 103°24′E with a combined drainage area of 130 000 km^2. The Yellow River Headwaters is a high-altitude basin with an elevation of 2 438～6 169 m and an average elevation of 4 473 m, representing an NW-SE banded basin landform, and the main landform of which is plateaus, mountains, and hilly plateaus[8]. The natural environment in Yellow River Headwaters is diverse with widely distributed alpine vegetation, where the main types of vegetation are alpine shrub, alpine meadow, and alpine grassland[9].

1.2 Data source and processing

The normalized vegetation index(NDVI) data used in this paper are MOD13Q1 from 2003 to 2017 obtained from NASA, with a temporal resolution of 16d and a spatial resolution of 1 km. The MODIS Reprojection Tool(MRT) technique was used to splice and reproject the remote sensing image. The NDVI band and the mask were extracted in ArcGIS. Given the presence of surface landscapes such as rivers, lakes, rocks and bare soil in the Yellow River Headwaters, where NDVI value is less than zero, the raster calculation tool in ArcGIS was used to remove non-vegetation areas by setting the pixel value as null. Finally, the Max Value Composition(MVC) method was used to obtain the monthly NDVI Value. April to October is the vegetation growing season in the Yellow River Headwaters, thus the annual average from April to October is regarded as the annual NDVI value. The multi-year average spatial distribution of NDVI in the growing season from 2003 to 2017 is shown in Fig. 1(a).

The meteorological data from 12 stations with daily precipitation and temperature from 2003 to 2017 were obtained from the China Meteorological Administration(CMA). The Yellow River Headwaters is located in the eastern part of the Qinghai-Tibet plateau with a significant elevation difference, where the precipitation and temperature represent an obvious vertical distribution trend[10]. Therefore, Inverse Distance Weighted(IDW) spatial interpolation based on the DEM correction method was used to process meteorological data[11]. The vertical lapse rate of temperature is an important factor affecting spatial interpolation accuracy[12]. A linear regression model was established by using the multi-year mean temperature($\overline{T}$) and monitoring station elevation(h) of 12 meteorological stations in the study area(Fig. 2). The regression

model equation of $\overline{T}$ and h is $\overline{T}=-0.005\,5h+21.41$ with the R^2 of 0.867 6, which determined the vertical decline rate of temperature to be −0.55 ℃ per 100 m.

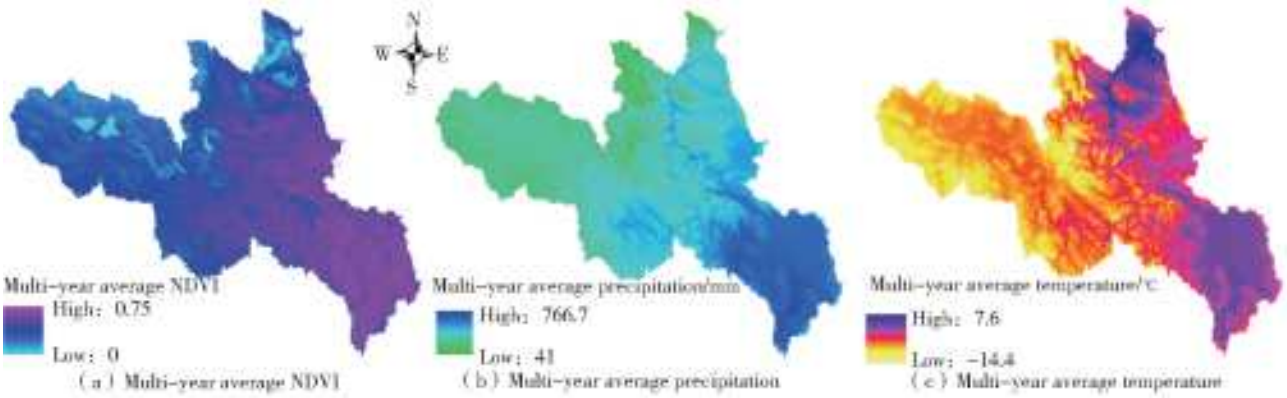

Fig. 1 Multi-year average spatial distribution of NDVI, temperature, and precipitation

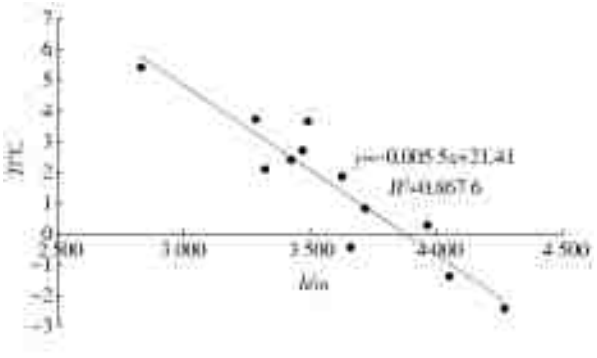

Fig. 2 Regression model for multi-year mean temperature and station elevation of meteorological stations

The annual precipitation in northwest China increases with the elevation, with a range of 1～18.13 mm/m[13]. Studies have shown that the precipitation on the Qinghai-Tibet plateau has gradient changes and the precipitation in the eastern region increases by 6～22 mm per 100 m[14-15]. Hao[16] analyzed the rain measuring station in the Yellow River Headwaters and concluded that the vertical change rate of precipitation was +20 mm/m. Therefore, the vertical change rate of precipitation was selected as +20 mm/m in this paper. Based on the vertical change rate of temperature and precipitation, the data of monitoring station were revised to the geoid, then IDW method was used to interpolate the meteorological data in ArcGIS and combined with DEM with a spatial resolution of 30 m, the temperature and precipitation data on the geoid were revised to the normal elevation. The spatial distribution of multi-year average temperature and multi-year average precipitation from 2003 to 2017 is shown in Fig. 1(b) and Fig. 1(c).

1.3 Correlation analysis

The correlation analysis between NDVI and temperature and precipitation in the Yellow River Headwaters from 2003 to 2017 was carried out. The correlation coefficient was denoted as R

$$R=\frac{\sum_{i=1}^{n}(X_i-\overline{X})(Y_i-\overline{Y})}{\sqrt{\sum_{1=1}^{n}(X_i-\overline{X})^2\sum_{i=1}^{n}(Y_i-\overline{Y})^2}} \quad (1)$$

where X_i is the NDVI in a given year; $\overline{T}$ is the multi-year average for NDVI; Y_i is the temperature or precipitation in a given year; $\overline{Y}$ is the multi-year average for temperature or precipitation; n is the length of study period which is 15.

t-test[17] was used to test the significance of the correlation, and the formula was as follows

$$t=R\Big/\sqrt{\frac{1-R^2}{n-2}} \quad (2)$$

where t and R are testing statistic and correlation coefficient, respectively. The grade was divided into 5 grades according to the correlation coefficient and significance test[18], which are extremely significant negative correlation ($R<0$, $P\leqslant 0.01$), significant negative correlation ($R<0$, $0.01<P\leqslant 0.05$), non-significant correlation ($P>0.05$), significant positive correlation ($R>0$, $0.01<P\leqslant 0.05$), and extremely significant positive correlation ($R>0$, $P\leqslant 0.01$).

1.4 Elevation section division

To study the distribution of NDVI with elevation in the Yellow River Headwaters, sample points at equal intervals in the research area were selected in ArcGIS to extract the elevation and the

multi-year average NDVI. As can be seen from the change diagram of NDVI with elevation(Fig. 3(a)). The NDVI value first represented a trend of increasing with elevation, then increased dramatically after reaching a certain altitude, followed by the trend of slowly decreasing with elevation, then represented scattered distribution after reaching a certain altitude. The *t*-test method was used to find the mutant point of NDVI with elevation. The Double population *t*-test is a method to test the mutation by examining whether the difference of the average value of two groups of non-correlated sample sequences is significant[19]. If the difference of the average of the two groups of samples exceeds the significance level, the two groups of samples are considered to have a mutation. The indexes were calculated as follows

$$t=\frac{\overline{X}_1-\overline{X}_2}{\sqrt{\frac{(n_1-1)S_1^2+(n_2-1)S_2^2}{n_1+n_2}\left(\frac{1}{n_1}+\frac{1}{n_2}\right)}} \tag{3}$$

where S_1^2 and S_2^2 are the variances of two samples, respectively; n_1 and n_2 are the averages of($\overline{X}_1$) and ($\overline{X}_2$), respectively. In this paper, the NDVI of the sample points was divided into one group per 100 m elevation, and every two groups of sample points were tested by double population *t*-test at a 95% confidence level to detect the mutation of NDVI with elevation. As can be seen from Fig. 3(b), there was a significant difference in NDVI between the two groups at altitudes of 3 300～3 400 m and 4 100～4 200 m, which can be considered that NDVI mutated at altitudes of 3 400 m and 4 200 m. Therefore, the elevation of 3 400 m was set as the first dividing line of the elevation section, and the elevation of 4 200 m was set as the second dividing line of the elevation section so that the whole study area was divided into three vertical sections of the section Ⅰ(<3 400 m), section Ⅱ(3 400～4 200 m) and section Ⅲ(>4 200 m).

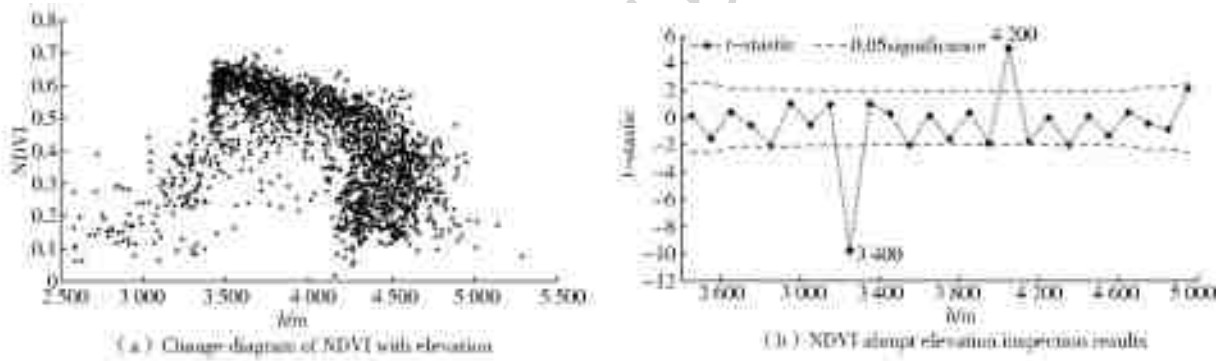

(a) Change diagram of NDVI with elevation (b) NDVI abrupt elevation inspection results

Fig. 3 NDVI distribution with elevation and mutation detection results

The schematic diagram of the elevation sections in the study area is shown in Fig. 4. Section Ⅰ is mainly located in the northeast of the study area, with an average elevation of 3 105 m and an area of 9 137 km^2, accounting for 7% of the total basin area, while the NDVI is distributed in[0.03, 0.5], with an average value of 0.26; Section Ⅱ is mainly located in the southeast of the study area, with an average elevation of 3 731 m and an area of 57 744 km^2, accounting for 45% of the total basin area, while NDVI is distributed in[0.26, 0.66], with an average value of 0.55; Section Ⅲ is located in the northwest of the study area, with an average elevation of 4 441 m and an area of 62 094 km^2, accounting for 48% of the total basin area, while NDVI is distributed in[0.09, 0.56], with an average value of 0.34.

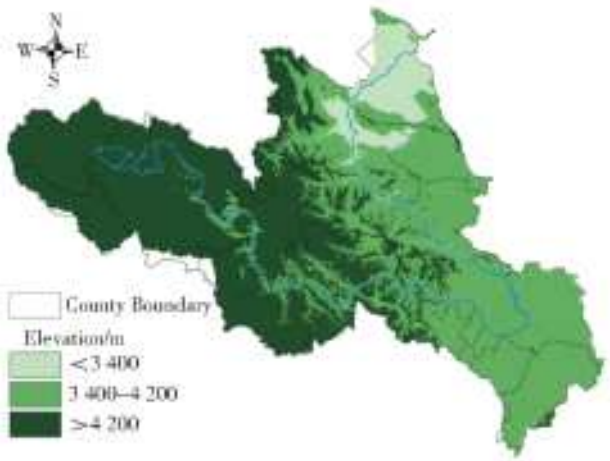

Fig. 4 Schematic diagram of the elevation sections

2 Results and discussion

2.1 Vegetation distribution patterns in different elevations

To study NDVI, we should first understand the distribution of vegetation in the research area. The land use maps of 2000 and 2015 were selected for the transfer matrix analysis, and the results showed that the change of forest and farmland area is less than 0.1% and that of the grassland area is less than 2%. It can be considered that the land use in the Yellow River Headwaters had barely changed from 2003 to 2017. Therefore, the land use maps of 2015 with a spatial resolution of 1km was chosen as a typical year to analyze the vegetation types in the Yellow River Headwaters. Fig. 5 shows that: the types of vegetation in the Yellow River Headwaters are grassland, forest, and farmland, the grassland is the main type accounting for 75% of the whole area, followed by the forest, which accounts for 7% of the whole area, while there is a small amount of farmland in the northeast, which covers only 1% of the study area.

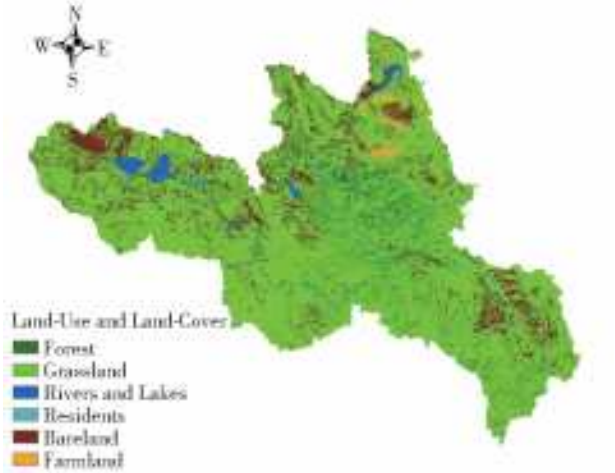

Fig. 5 The Land-use map of the study area in 2015

The land use map was superimposed with the elevation sections to obtain the proportions of different vegetation types in different elevation sections(Fig. 6). The vegetation area(forest, grassland and farmland) accounts for 73.39% of the total land-use area in section Ⅰ, where the main types of vegetation are Farmland and grassland, accounting for 16.79% and 79.46%, respectively, and forest land accounts for 3.75%; The vegetation area accounts for 87.52% of the total land-use area in section Ⅱ, where the main types of vegetation are forest and grassland, accounting for 14.25% and 85.61%, respectively. The vegetation area accounts for 78.82% of the total land-use area in section Ⅲ, 97.02% of which is grassland, and the forest only accounts for 2.98%.

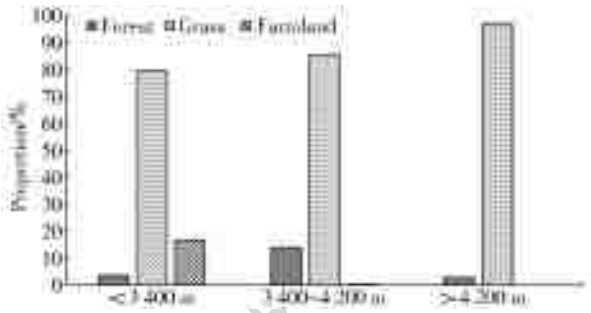

Fig. 6 The proportion of different vegetation types in different elevation sections

NDVI is closely related to many parameters of vegetation, which can reflect vegetation differences and vegetation growth trends[20]. Therefore, the NDVI of different types of vegetation differ. Kernel density estimation probability distribution is a non-parametric estimation method that can reflect the distribution of samples[21]. Three types of vegetation(forest-L, grassland-C, and farmland-T) were extracted and their annual average NDVI values were estimated for kernel density distribution to explore the distribution characteristics of NDVI of different types of vegetation(Fig. 7).

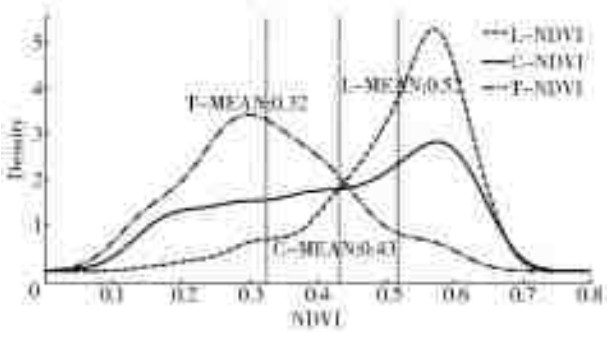

Fig. 7 Kernel density estimation distribution of forest, grassland, and farmland

It can be seen from the comparison that the average NDVI of the forest is 0.52, which is the highest, followed by grassland, which is 0.43 and that of farmland is 0.32 which is the smallest. The distribution characteristics of NDVI in the three vegetation represents diversity. The distri-

bution of NDVI in forest is relatively concentrated, that in grassland is relatively uniform with a large span, and that in farmland is close to the normal distribution. According to the determination of upper and lower limits of 95% confidence interval, the distribution range of NDVI in forest is [0.27, 0.65], that in grassland is [0.14, 0.64], and that in farmland is [0.13, 0.57], which conclude that regional differences in the distribution of vegetation types caused the characteristics of NDVI changing with elevation. NDVI in section Ⅰ mainly represents the farmland and grassland, where NDVI is small; NDVI in section Ⅱ mainly represents the forest and grassland, where NDVI is higher; NDVI in section Ⅲ only represents the grassland. These may explain why NDVI is scattered.

2.2 Hydrothermal conditions in different elevations

Precipitation and temperature are two important meteorological factors affecting the vegetation cover[22]. The joint distribution map of the multi-year average hydrothermal conditions from 2003 to 2017 in three elevation sections(Fig. 8) were drawn to explore the causes of the spatial distribution difference of NDVI in the Yellow River Headwaters. The distribution range of precipitation in section Ⅰ is(286 mm, 587 mm), while concentrated between 400 mm and 500 mm. The temperature distribution range in this region is(1.5 ℃, 6.9 ℃), and concentrated between 3 ℃ and 5 ℃; The distribution of precipitation in section Ⅱ is relatively uniform, ranging from 320 mm to 717 mm with an average of 553 mm. The temperature distribution span is large and presents a the bimodal type in this region, ranging from 3.2 ℃ to 3.08 ℃ with an average of 0.34 ℃ but concentrated between 2 ℃ and 4 ℃ and between −1 ℃ and 1 ℃; The distribution of precipitation in section Ⅲ is relatively concentrated, with the range of 241 mm to 533 mm and an average of 377 mm, while concentrated between 250 mm and 350 mm. The temperature distribution in this region ranges from 6.6 ℃ to 1.7 ℃ with an average of 3.87 ℃. The spatial distribution pattern of temperature is gradient decreasing, and the thermal condition follows the law of altitude decreasing with the elevation. While precipitation is decreasing from southeast to northwest. This is because the Indian Ocean and the Pacific Ocean are the main sources of water vapor in the eastern part of the Qinghai-Tibet plateau[23]. From the point of hydrothermal conditions, section Ⅰ belongs to the arid region with high temperature and less precipitation, and section Ⅱ belongs to the moist-heat region with high temperature and much precipitation, and section Ⅲ belongs to the dry region with low temperature and little precipitation. Section Ⅱ has the relatively best hydrothermal conditions, which is followed by Section Ⅰ, while Section Ⅲ is the worst of three partitions.

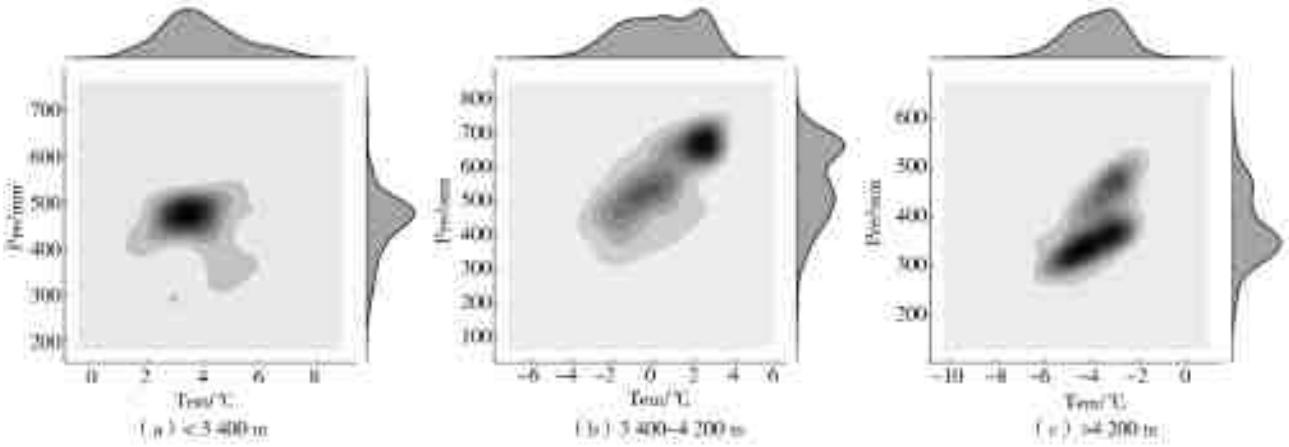

Fig. 8 Comparison of distribution characteristics of hydrothermal conditions at different elevation sections

2.3 NDVI responds to the hydrothermal factor in different elevations

The correlation analysis of annual NDVI value, temperature and precipitation from 2003 to 2017 was carried out respectively, and its significance was tested by *t*-test. The spatial distribution

diagram and statistical results of the correlation between NDVI and hydrothermal factors in different elevation sections were shown in Fig. 9 to 10. The results show that the vegetation and climate factors in most areas of the basin were non-significant correlation or significantly positively correlated, and few areas were significantly negatively correlated, but almost none were extremely significant negative correlation. There are differences in the factors that have a significant influence on NDVI in different elevation sections. In section Ⅰ, the areas where NDVI is positively correlated with precipitation account for 59.3%, but only 4.3% are positively correlated with temperature. In section Ⅱ, 12.6% of NDVI was positively correlated with precipitation, while 44.1% of NDVI was positively correlated with temperature. There is a positive correlation between NDVI and precipitation in 43.4% of regions in section Ⅲ, but only 8.2% of regions with a positive correlation between NDVI and temperature. Section Ⅰ and section Ⅲ show similar characteristics that NDVI has a good correlation with precipitation and a poor correlation with temperature, while section Ⅱ shows the opposite characteristic that NDVI has a higher correlation with temperature than with precipitation.

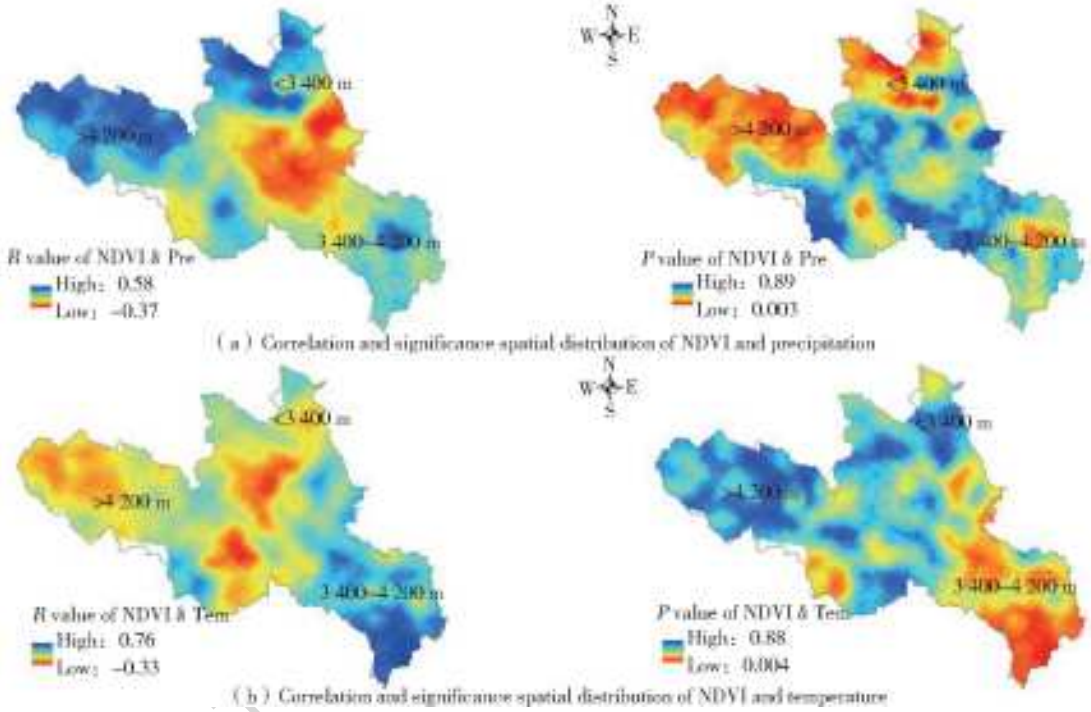

Fig. 9 Spatial distribution of correlation and significance between NDVI and hydrothermal factors

Fig. 10 Statistical results of correlation between NDVI and hydrothermal factors

Combined with the analysis of the distribution pattern of hydrothermal conditions in the three elevation segments in the previous section, it can be found that NDVI is driven by different hydrothermal factors with different natural conditions. The main factor that affects the growth of vegetation in section I and Ⅲ where the precipitation is less, while that is the temperature in Section II where the rainfall is abundant. The reasons for this result may be that the climate of section I and Ⅲ in the north is characterized by drought, water scarcity, and low soil water content, where vegetation growth is greatly restricted by water. The increase of precipitation can increase soil moisture, which can provide sufficient water for the growth of vegetation, and promote the photosynthesis of plants. Therefore, NDVI and precipitation are positively

correlated in these two elevation sections. And for section Ⅱ with abundant precipitation and high soil moisture content, vegetation growth will not be restricted by water conditions so that the influence of precipitation on the growth of vegetation will be weakened, and then the temperature will become the main factor affecting the growth of vegetation.

3 Conclusion

In this paper, the distribution pattern of vegetation and hydrothermal conditions were analyzed, and the correlation between NDVI and hydrothermal factors was investigated based on three elevation sections The main conclusions are as follows.

(1) The main type of vegetation is farmland and grassland distributed in section Ⅰ, and that are forest and grassland distributed in section Ⅱ, while there is the only grassland distributed in section Ⅲ. The NDVI of different vegetation types shows different distribution characteristics. The NDVI distribution of forest is relatively concentrated, while that of grassland is relatively uniform with a large span, and that of farmland is close to normal distribution. The average NDVI of different vegetation types ranks in this order: forest>grassland>farmland.

(2) The temperature represents a spatial distribution pattern of gradient decline, and the precipitation represents a trend of decline from southeast to northwest. Section Ⅰ belongs to the arid region with high temperature and less precipitation, and section Ⅱ belongs to the moist-heat region with high temperature and much precipitation, and section Ⅲ belongs to the dry region with low temperature and little precipitation. Section Ⅱ has the relatively best hydrothermal conditions, which is followed by section Ⅰ, while section Ⅲ is the worst of three partitions.

(3) NDVI is driven by different hydrothermal factors in different sections. The main factor that affects the growth of vegetation in section I and Ⅲ is precipitation where the precipitation is less, while that is the temperature in section II where the rainfall is abundant.

References:

[1] HE X J, WANG G Q, BAO Z X. Progress and prospective of climate and vegetation coverage change as well as responses of hydrological cycle[J]. Journal of Water Resources and Water Engineering, 2016, 27(2): 1-5. (in Chinese) DOI: 10. 11705/j. issn. 1672-643X. 2016. 02. 01.

[2] LIU Q X, DONG G T, JING H T, et al. Change trend of vegetation NDVI and its influencing factors in the source region of the Yellow River in the period from 2000 to 2016[J]. Research of Soil and Water Conservation, 2019, 26(3): 86-92. (in Chinese) DOI: 10. 13869/j. cnki. rswc. 2019. 03. 013.

[3] LAN Y C, LU C Y, LA C F, et al. The fact of climate shift to warm-humid in the source regions of the Yellow River and its hydrologic response[J]. Journal of Glaciology and Geocryology, 2013, 35(4): 920-928. (in Chinese) DOI: 10. 7522/j. issn. 1000 0240. 2013. 0104.

[4] XU H J, YANG T B, ZENG B. Spatial-temporalvariation of growing-season NDVI and its responses to climate change over the source region of the Yellow River [J]. Ecology and Environmental Sciences 2012, 21(7): 1205-1210. (in Chinese) DOI: 10. 3969/j. issn. 1674-5906. 2012. 07. 005.

[5] SHI D D, YANG T, HU J M, et al. Spatio-temporal variation of NDVI-based vegetation during the growing-season and its relation with climatic factors in the Yellow River source region[J]. Mountain Research, 2018, 36(2): 184-193. (in Chinese) DOI: 10. 16089/j. cnki. 1008-2786. 000314.

[6] WU X F, LI G X, PAN X P, et al. Response of vegetation cover to temperature and precipitation in the source region of the Yellow River[J]. Resources Science, 2015, 37(3): 512-521. (in Chinese)

[7] HU G Y, JIN H J, DONG Z B, et al. Research of land-use and land-cover change (LUCC) in the source regions of the Yellow River[J]. Journal of Glaciology and Geocryology, 2014, 36(3): 573-581. (in Chinese) DOI: 10. 7522issn. 10000240. 2014. 0068.

[8] QIAN C, HAN J E, ZHU D G, et al. Structural and geomorphic analysis of the Yellow River source region based on ASTER-GDEM data[J]. Geology in China, 2012, 39(5): 1247-1260. (in Chinese) DOI: 10. 3969/j. issn. 1000-3657. 2012. 05. 012.

[9] CHEN Q, ZHOU Q, ZHANG H F, et al. Spatial disparity of NDVI response in vegetation growing season to climate change in the Three-River Headwaters[J]. Region Ecology and Environmental Sciences, 2010, 19(6): 1284-1289. (in Chinese) DOI: 10. 3969/j. issn. 1674-5906. 2010. 06. 004.

[10] ZHANG J, LI D L, HE J M, et al. Influence of terrain

on precipitation distribution in Qingzang tableland in wet and dry years[J]. Advances in Water Science, 2007(3):319-326. (in Chinese) DOI:10.3321/j.issn:1001-6791.2007.03.002.

[11] CUI X L, CHEN Z, ZHANG L, et al. Spatial interpolation of MODIS surface temperature products based on DEM correction[J]. Journal of Geo-Information Science, 2018, 20(12):1768-1776. (in Chinese) DOI:10.12082/dqxxkx.2018.180340.

[12] CAI D H, GUO N, LI C W. Interpolation of air temperature based on DEM[J]. Journal of Arid Meteorology, 2009, 27(1):10-17. (in Chinese) DOI:10.3969/j.issn.1006-7639.2009.01.002.

[13] XUAN H Y, LUO S H. Analyses of the relationships between the precipitation and ltitude of China[C]. Proceedings of the 13th Annual Conference of China Society of Field Statistics, 2007:110-113. (in Chinese)

[14] LU C X, WANG L, XIE G D, et al. Altitude effect of precipitation and spatial distribution of Qinghai-Tibetan Plateau[J]. Journal of Mountain Science, 2007(6):655-663. (in Chinese) DOI:10.3969/j.issn.1008-2786.2007.06.003.

[15] LU C X, YU G, GUO G M, et al. Altitude effect of precipitation and water tower effect of Qinghai-Tibetan Plateau[C]. Abstracts of 2005 Qinghai-Tibet Plateau Environment and Change Conference, 2005:17. (in Chinese)

[16] HAO Z C, ZHANG Y G, YANG C G, et al. Effects of topography and snowmelt in hydrological modeling of the source region of the Yellow River[J]. Advances in Water Science, 2013, 24(3):311-318. (in Chinese)

[17] CHEN Y G. Geographic mathematical method[M]. Beijing: Science Press, 2011. (in Chinese)

[18] GAO Q Z, LI Y, WAN Y F, et al. Dynamics of alpine grassland NPP and its response to climate change in northern Tibet[J]. Climatic Change, 2009, 97(3-4):515. DOI:10.1007/s10584-009-9617-z.

[19] WEI F Y. Modern techniques of climate statistical diagnosis and prediction[M]. Beijing: Meteorological Press, 2007. (in Chinese)

[20] CHEN Z H, ZHU J, XU X K. Recent research progress in uncertainties of the normalized difference vegetation index, land cover classification and vegetation fraction estimation climatic and environmental research[J]. Climatic and Environmental Research, 2004(4):687-696. (in Chinese) DOI:10.3969/j.issn.1006-9585.2004.04.013.

[21] NA L, QIAN F. Multi-objective evolutionary of distribution algorithm using kernel density estimation model[C]. Proceedings of the 8th World Congress on Intelligent Control and Automation. 2010:2843-2848. DOI:10.1109/WCICA.2010.5554745.

[22] XU X K, LIN Z H, XU F, et al. Correlation analysis between meteorological factors and the ratio of vegetation cover[J]. Acta Ecologica Sinica, 2003(2):221-230. (in Chinese) DOI:10.3321/j.issn:1000-0933.2003.02.001.

[23] ZHANG W J, GAO Z Q. Spatial variation of water/thermal elements and NDVI with altitudes in central and eastern Tibetan Plateau[J]. Geographical Research, 2006(5):877-886. (in Chinese) DOI:10.3321/j.issn:1000-0585.2006.05.01.